APPLIED PHYSICS LETTERS VOLUME 81, NUMBER 14 30 SEPTEMBER 2002

Raman characterization of boron-doped multiwalled carbon nanotubes

J. Maultzsch,[a] S. Reich, and C. Thomsen
Institut für Festkörperphysik, Technische Universität Berlin, Hardenbergstrasse 36, 10623 Berlin, Germany

S. Webster, R. Czerw, and D. L. Carroll
School of Materials Science and Engineering, Clemson University, Clemson, South Carolina 29634

S. M. C. Vieira, P. R. Birkett, and C. A. Rego
Department of Chemistry and Materials, Manchester Metropolitan University, Chester Street, M1 5QP, United Kingdom

(Received 28 May 2002; accepted 12 August 2002)

We present first- and second-order Raman spectra of boron-doped multiwalled carbon nanotubes. The Raman intensities are analyzed as a function of the nominal boron concentration. The intensities of both the *D* mode and the high-energy mode in the first-order spectra increase with increasing boron concentration, if normalized with respect to a second-order mode. We interpret this result as an indication that the high-energy mode in carbon nanotubes is defect-induced in a similar way as the *D* mode. Based on this result, we provide a preliminary quantitative relation between the boron concentration and the Raman intensity ratios. © *2002 American Institute of Physics.*

[DOI: 10.1063/1.1512330]

Carbon nanotubes are promising systems for the fabrication of molecular electronic devices, such as transistors and logic circuits.[1–5] These devices require precise control of the electronic properties of the tubes, which is achieved by doping, for example, with alkali metals to increase the conductivity.[6–8] While alkali metals intercalate into the nanotube material, boron and nitrogen as dopants are expected to substitute for the carbon atoms.[9–11] Raman spectroscopy is, among others, often used to characterize the structural and electronic properties of the doped sample as well as the nature of the doping process.[12–15] Conversely, doping the material allows to control the defect concentration and can thus be used for further investigating the Raman processes in carbon nanotubes, which are most sensitive to the presence of defects. The so-called *D* mode at around 1300 cm^{-1} in the first-order Raman spectra of carbon nanotubes and graphite is induced by disorder in a double-resonant Raman process.[16,17] When estimating the defect concentration, the *D*-mode intensity is usually normalized with respect to the intensity of the high-energy mode (HEM, often called *G* mode) at around 1600 cm^{-1} (see, e.g., Refs. 18 and 19). This approach relies on the assumptions that, (i) the intensity of the high-energy mode is independent of the defect concentration and (ii) the intensity ratio does not depend on any other effects. On the other hand, if the high-energy mode itself is defect-induced, as was suggested in Ref. 20, this procedure for normalizing the intensity is no longer correct. Instead, both first-order modes should exhibit a (possibly different) intensity dependence on the defect concentration. This can be investigated by normalizing the first-order modes with respect to a second-order overtone mode whose intensity *per se* does not depend on the presence of defects (except for those effects that affect first- and higher-order scattering equally).

In this article, we present first- and second-order Raman spectra of boron-doped multiwalled carbon nanotubes (MWNT) at different doping levels. By normalizing the intensity of the first-order peaks with respect to the second-order overtone mode D^*, we show that not only the *D* mode but also the high-energy mode depends on the defect concentration. We give a tentative quantitative relation between the Raman-intensity ratios and the nominal boron concentration. Furthermore, our results support the interpretation of the high-energy mode in carbon nanotubes as being determined by a defect-induced, double resonant process.[20]

The samples were prepared by the arc-discharge method where the anode rod is doped with varying weight concentrations of boron as described elsewhere.[21] Raman measurements were performed with a Renishaw 1000 Ramascope; Stokes spectra were taken at an excitation wavelength of 785 nm.

In Fig. 1 we show the first- and second-order Raman spectra at three different doping levels. The spectra are normalized with respect to laser power and integration time. We find the absolute intensity of the *D* mode in the doped samples to be roughly constant; it increases slightly from 0.5% to 1% nominal boron concentration and decreases again at 4% nominal boron concentration. The high-energy mode as well as the D^*-mode intensities decrease with increasing defect concentration; the D^*-mode intensity decreases much faster than the HEM intensity.

In general, the absolute Raman intensities can change because of a different absorption cross section in the disordered sample. Another general effect of disorder is the reduction of the crystal symmetry, which leads to a softening of the $q \approx 0$ rule for first-order scattering or the $q_1 \pm q_2 \approx 0$ rule in second order and results in a broadening of the Raman peaks.[22,23] These mechanisms have, in general, a similar influence on first- and second-order intensities. On the other hand, there are additional effects which selectively enhance particular first-order modes. First, Γ-point phonon modes,

---

[a] Electronic mail: janina@physik.tu-berlin.de

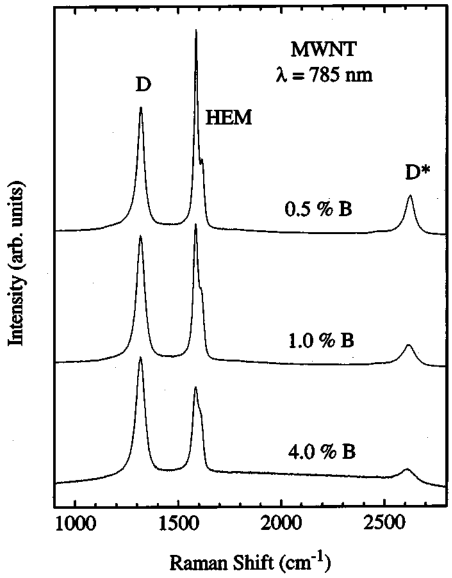

FIG. 1. First- and second-order Raman spectra of MWNT with different nominal boron concentrations. The intensities have been normalized with respect to laser power and integration time.

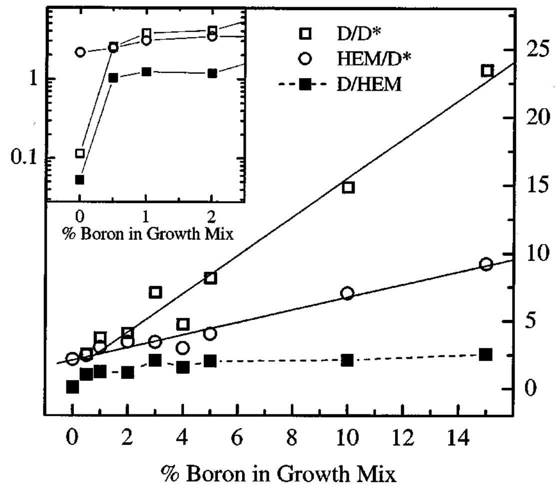

FIG. 2. Relative Raman intensities as a function of nominal boron concentration. The intensity is found by fitting each Raman mode separately by one or two Lorentzians and taking the total peak area. Closed symbols indicate the intensity ratio *D*/HEM; open squares and circles indicate the intensity of the *D* mode and the HEM, respectively, normalized to the *D** mode intensity. The solid lines are linear fits to the data; the dashed line is a guide to the eye. Inset: semi-logarithmic plot of the region of low boron concentration.

which are forbidden by symmetry in the perfect crystal, can become allowed and appear in the Raman spectra. Second, because the $q \approx 0$ rule no longer applies, particular phonon modes from inside the Brillouin zone can contribute with a strong Raman signal in a double resonance process. In carbon nanotubes, in particular, the latter is the dominating process in Raman scattering. Thus, a large defect concentration might lead to an increased scattering cross section for any defect-induced, double-resonant Raman mode in the first-order spectra of carbon nanotubes. The second-order signal, on the other hand, is caused by a double-resonant process in carbon nanotubes, independently of the presence of defects. Therefore, by normalizing the first-order intensities with respect to the second-order overtone mode D^* we can distinguish between first-order modes that are defect-induced and enhanced through a double resonance and Γ-point modes that are not enhanced by defects.

In Fig. 2 we show the relative intensities of the Raman peaks as a function of the nominal boron concentration. Open squares and open circles indicate the intensity of the *D* mode and the high-energy mode, respectively, normalized with respect to the second-order overtone D^* of the *D* mode. As expected for a disorder-induced mode, the relative intensity of the *D* mode increases with increasing number of defects. Between 0% and 0.5% nominal boron concentration, the intensity ratio D/D^* increases rapidly (by a factor of 25, see inset of Fig. 2); for higher concentrations the increase is weaker. The relative intensity of the high-energy mode increases as well with increasing nominal boron concentration, although at a somewhat lower rate than the *D* mode. This behavior is contrary to what is expected for a first-order, Raman-allowed Γ-point mode, whose intensity should exhibit the same dependence on the concentration of defects as the second-order overtone modes. The only exception is a defect-induced scattering process, in which phonon wave vectors $q > 0$ become involved and allow a double-resonance process that selectively enhances particular first-order modes. This does not affect the second-order spectra, since in second-order scattering all phonon wave vectors throughout the Brillouin zone are allowed, independent of the defect concentration. Therefore, the increasing intensity ratio HEM/D^* indicates that, besides the *D* mode, the high-energy mode in carbon nanotubes is disorder-induced (for multiwalled tubes at least in part) as well.[20]

In order to estimate the defect concentration, usually the intensity ratio *D*/HEM is investigated. This is shown by the closed squares in Fig. 2. Indeed, the intensity of the *D* mode compared to the HEM intensity increases as well, but the increase is rather weak above 3% nominal boron concentration. As shown above, the intensity of the high-energy mode itself depends on the number of defects in the sample; it is thus not appropriate as a basis for normalization. Instead, we can use both intensity ratios, D/D^* and HEM/D^*, to find a correlation between the boron concentration and the Raman intensities. We approximate the relative intensities with linear functions (see Fig. 2) for the relative intensities and obtain $I^{D/D^*} = 1.3 + x \cdot 1.4(\%\ \mathrm{conc.})^{-1}$ between 1% and 15% and $I^{\mathrm{HEM}/D^*} = 2.1 + x \cdot 0.47(\%\ \mathrm{conc.})^{-1}$ between 0% and 15% B concentration, where x is the nominal boron concentration.[24] Note that at this point we do not know the actual boron concentration, but only the nominal concentration as given by our growth parameters. Determination of the actual boron concentrations and their quantitative correlation to the Raman intensities is subject to future work.

If both the *D* mode and the high-energy mode result from a defect-induced Raman process, the question arises, why the increase in relative intensity HEM/D^* is much weaker (at least at the lowest doping levels) than the increase of the ratio D/D^* (inset of Fig. 2). This behavior can be understood from the different phonon wave vectors that give rise to the *D* and high-energy modes, respectively. According to the double-resonance description, the HEM phonon wave vectors are rather close to the Γ point compared to those of the *D* mode. [20] Thus even a low defect concentration leads to a weak spatial confinement of the high-energy phonon modes. The corresponding distribution of phonon wave vectors is large enough to allow those near-Γ-point modes, which fulfill the double-resonance condition, to contribute to the scattering process. For example, let the defect concentration be 0.1%, that is, there is one defect per 1000 carbon atoms. In the (10, 10) tube this results in one defect in 25 unit cells or a mean distance between the defects of $25a_0$, where a_0 is the length of the graphene lattice vectors. The wave vector corresponding to the mean distance between the defects is $k=2\pi/(25a_0)=0.08\pi/a_0$, which is already large compared with the wave vector of visible light (on the order of $10^{-3}\pi/a_0$). In the (20, 20) tube, the same defect concentration leads to a mean distance between the defects of $12.5a_0$ or a corresponding wave vector $k=0.16\pi/a_0$. For tubes of similar diameter but different chirality, the mean distance between the defects varies only slightly at a given defect concentration. Since the phonon wave vectors that fulfill the double-resonance condition for the high-energy modes are all in the range of $0.1-0.3\pi/a_0$ (independent of the chirality of the tube), these modes originate from a double-resonance Raman process already at a low defect concentration. On the other hand, the phonon wave vectors leading to the *D* mode are large compared to those of Γ-point modes. A low defect concentration thus affects the *D* mode intensity much less than the HEM intensity. When the number of defects increases, the mean distance between the defects eventually becomes comparable with the wavelength of the *D* mode phonons. At this point, the *D* mode intensity increases rapidly as it benefits strongly from the enhancement of the defect concentration. The long-wavelength phonon modes in the high-energy Raman peak, on the other hand, are now less influenced by the increasing number of defects and exhibit only a weak enhancement in intensity. In this way we can understand the initial stronger increase of the *D*-mode signal as compared to that of the HEM.

In conclusion, we presented the intensity dependence of first-and second-order Raman modes of multiwalled carbon nanotubes on the defect concentration. We demonstrated that the intensity of both the *D* mode and the high-energy mode, if normalized to the second-order mode D^*, increases with the density of the defects in the sample. Therefore, normalizing the *D* mode intensity with respect to the high-energy mode intensity is not suitable for estimating the defect concentration in carbon nanotube samples. Instead, a better procedure to obtain information on the relative number of defects is to normalize the intensity of the first-order modes to the second-order overtone modes. In addition, our results support the interpretation that the high-energy mode, which is usually regarded as a Raman-allowed Γ-point mode, in fact originates from the same defect-induced, double-resonant process as the *D* mode, although involving comparatively small phonon wave vectors.

This work was supported by the Deutsche Forschungsgemeinschaft under Grant No. Th 662/8-1 and by AFOSR under Grant No. F49620-99-1-0173 (US).

[1] S. J. Tans, A. Verschueren, and C. Dekker, Nature (London) **393**, 6680 (1998).
[2] R. Martel, T. Schmidt, H. R. Shea, T. Hertel, and Ph. Avouris, Appl. Phys. Lett. **73**, 2447 (1998).
[3] H. W. C. Postma, T. Teepen, Z. Yao, M. Grifoni, and C. Dekker, Science **293**, 76 (2001).
[4] V. Derycke, R. Martel, J. Appenzeller, and Ph. Avouris, Nano Lett. **1**, 453 (2001).
[5] A. Bachtold, P. Hadley, T. Nakanishi, and C. Dekker, Science **294**, 1317 (2001).
[6] R. S. Lee, H. J. Kim, J. E. Fischer, A. Thess, and R. E. Smalley, Nature (London) **388**, 255 (1997).
[7] V. Derycke, R. Martel, J. Appenzeller, and P. Avouris, Appl. Phys. Lett. **80**, 2773 (2002).
[8] X. Liu, C. Lee, C. Zhou, and J. Han, Appl. Phys. Lett. **79**, 3329 (2001).
[9] O. Stephan, P. M. Ajayan, C. Colliex, P. Redlich, J. M. Lambert, P. Bernier, and P. Lefin, Science **266**, 1683 (1994).
[10] D. L. Carroll, P. Redlich, X. B. J.-C. Charlier, S. Curran, P. M. Ajayan, S. Roth, and M. Rühle, Phys. Rev. Lett. **81**, 2332 (1998).
[11] B. Wei, R. Spolenak, P. Kohler-Redlich, M. Rühle, and E. Arzt, Appl. Phys. Lett. **74**, 3149 (1999).
[12] A. M. Rao, P. C. Eklund, S. Bandow, A. Thess, and R. E. Smalley, Nature (London) **388**, 257 (1997).
[13] A. Claye, S. Rahman, J. E. Fischer, A. Sirenko, G. U. Sumanasekera, and P. C. Eklund, Chem. Phys. Lett. **333**, 16 (2001).
[14] N. Bendiab, A. Righi, E. Anglaret, J. L. Sauvajol, L. Duclaux, and F. Béguin, Chem. Phys. Lett. **339**, 305 (2001).
[15] W. Zhou, S. Xie, L. Sun, D. Tang, Y. Li, Z. Liu, L. Ci, P. Tan, X. Dong, B. Xu, and B. Zhao, Appl. Phys. Lett. **80**, 2553 (2002).
[16] J. Maultzsch, S. Reich, and C. Thomsen, Phys. Rev. B **64**, 121407(R) (2001).
[17] C. Thomsen and S. Reich, Phys. Rev. Lett. **85**, 5214 (2000).
[18] M. Hirscher, M. Becher, M. Haluska, U. Dettlaff-Weglikowska, A. Quintel, G. Duesberg, Y.-M. Choi, P. Downes, M. Hulman, S. Roth, I. Stepanek, and P. Bernier, Appl. Phys. A: Mater. Sci. Process. **72**, 129 (2001); L. Zhang, H. Li, K.-T. Yue, S.-L. Zhang, X. Wu, J. Zi, Z. Shi, and Z. Gu, Phys. Rev. B **65**, 073401 (2002).
[19] C. Zhi, X. D. Bai, and E. G. Wang, Appl. Phys. Lett. **80**, 3590 (2002).
[20] J. Maultzsch, S. Reich, and C. Thomsen, Phys. Rev. B **65**, 233402 (2002).
[21] S. M. C. Vieira, R. Czerw, S. Webster, P. R. Birkett, C. A. Rego, and D. L. Carroll (unpublished).
[22] M. H. Brodsky, in *Light Scattering in Solids I: Introductory Concepts*, edited by M. Cardona, *Topics in Applied Physics*, 2nd ed. Vol. 8 (Springer, Berlin, 1983), p. 205.
[23] R. S. Berg and P. Y. Yu, Phys. Rev. B **35**, 2205 (1987).
[24] For other spectrometers and excitation energies the numbers have to be corrected for the relative detector sensitivity S_{1st}/S_{2nd} at detection of the first and the second-order modes. In our experiments, this sensitivity ratio $S_{\mathrm{HEM}}/S_{D*}=2.5$.